2. PHYSICAL CHARACTERISTICS OF WASTE AREA GROUP 4

This section describes the physical geography, meteorology, geology, hydrology, demography, and ecology of WAG 4. Regional and local characteristics are also discussed.

2.1 Physiography

The INEEL, located on the northern edge of the Eastern Snake River Plain (ESRP), has an 80 to 112 km (50 to 70 mi) wide, northeastern-trending basin extending from the vicinity of Bliss, Idaho on the southwest to the Yellowstone Plateau on the northeast. Three mountain ranges end at the northern and northwestern boundaries of the INEEL: the Lost River Range, the Lemhi Range, and the Beaverhead Mountains of the Bitterroot Range. There are 1,188 to 1,306 m (3,960 to 4,620 ft) of relief between the ranges and the relatively flat plain (Hull 1989). Saddle Mountain Peak, near the southern end of the Lemhi Range, reaches an altitude of 3,243 m (10,810 ft) and is the highest point in the immediate area of the INEEL. The physiographic features of the INEEL area are shown in Figure 2-1.

The ESRP slopes upward from an elevation of approximately 750 m (2,500 ft) at the Oregon border, to over 1,500 m (5,000 ft) at Ashton, northeast of the INEEL. The ESRP is composed of two structurally dissimilar segments, with the division occurring between the towns of Bliss and Twin Falls, Idaho. East of Twin Falls, the Snake River has cut a valley through Tertiary basin fill sediments and interbedded volcanic rocks. The stream drainage is well developed, except in a few areas covered by recent thin basalt flows. The complexion of the plain changes as the Snake River flows further west through a vertical-walled canyon through thick sequences of Quaternary basalt with few interbedded sedimentary deposits.

The portion of the ESRP occupied by the INEEL may be divided into three minor physical provinces. The first province is a central trough, often referred to as the Pioneer Basin, that extends to the northeast through the INEEL. Two flanking slopes descend to the trough, one from the mountains to the northwest and the other from a broad ridge on the plain to the southeast. The slopes on the northwestern flank of the trough are mainly alluvial fans originating from sediments of Birch Creek and the Little Lost River. Also forming these gentle slopes are basalt flows that have spread onto the plain. The landforms on the southeast flank of the trough are formed by basalt flows, which spread from an eruption zone that extends northeastward from Cedar Butte (Figure 2-1). The lavas that erupted along this zone built up a broad topographic swell directing the Snake River to its current course along the southern and southeastern edges of the plain (Figure 2-2). This topographic swell effectively separates the drainage from mountain ranges northwest of the INEEL from the Snake River.

The central lowland of the INEEL broadens to the northeast and joins the extensive Mud Lake Basin. The Big and Little Lost Rivers and Birch Creek drain into this trough from valleys between the mountains to the north and west. The intermittently flowing waters of the Big Lost River have formed a flood plain in this trough, consisting primarily of fine sands, silts, and clays. The streams flow to the Lost River and Birch Creek Sinks and form a system of playa depressions in the west-central portion of the INEEL.

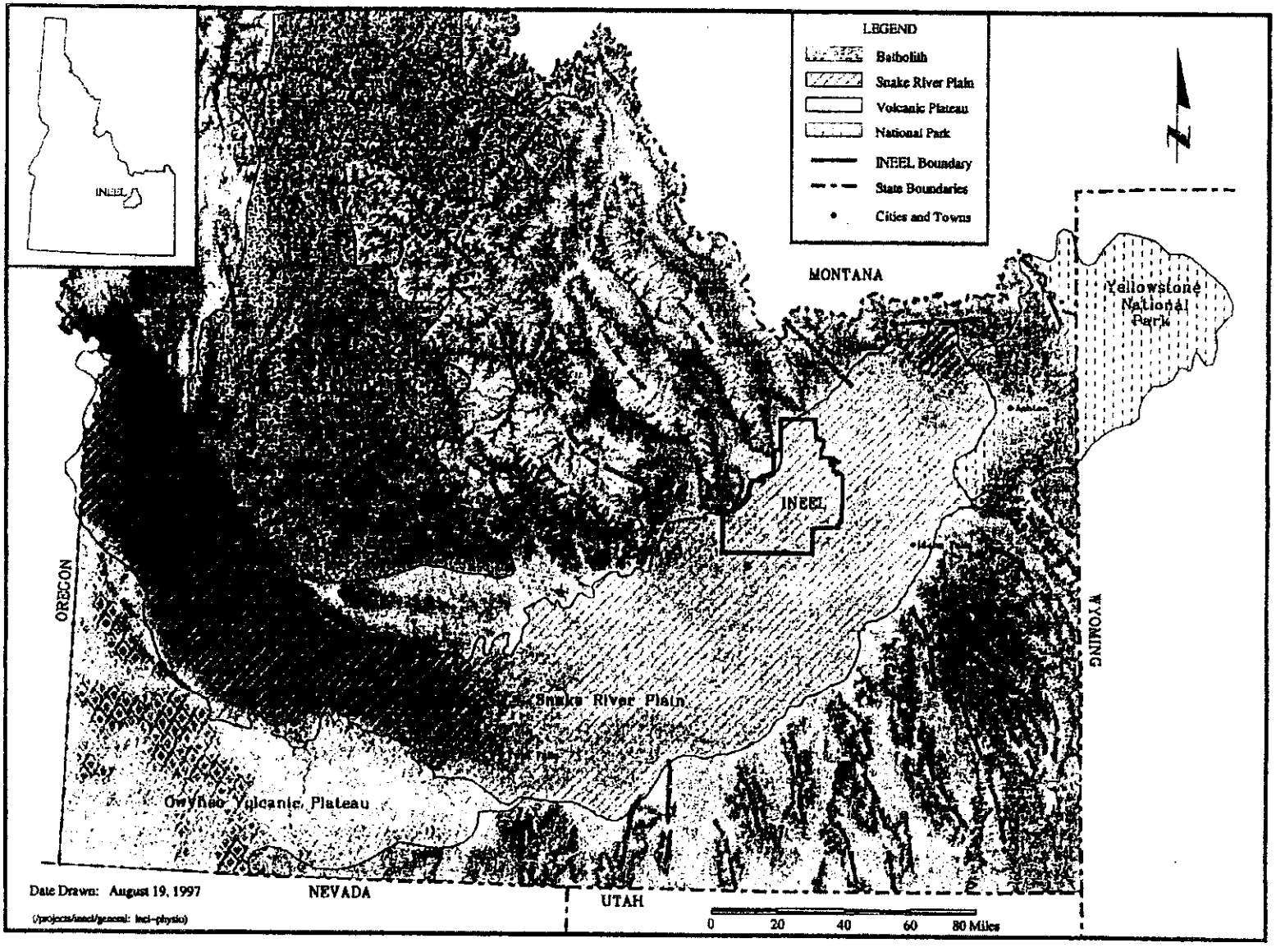

Figure 2-1. Physiographic features of the INEEL area.

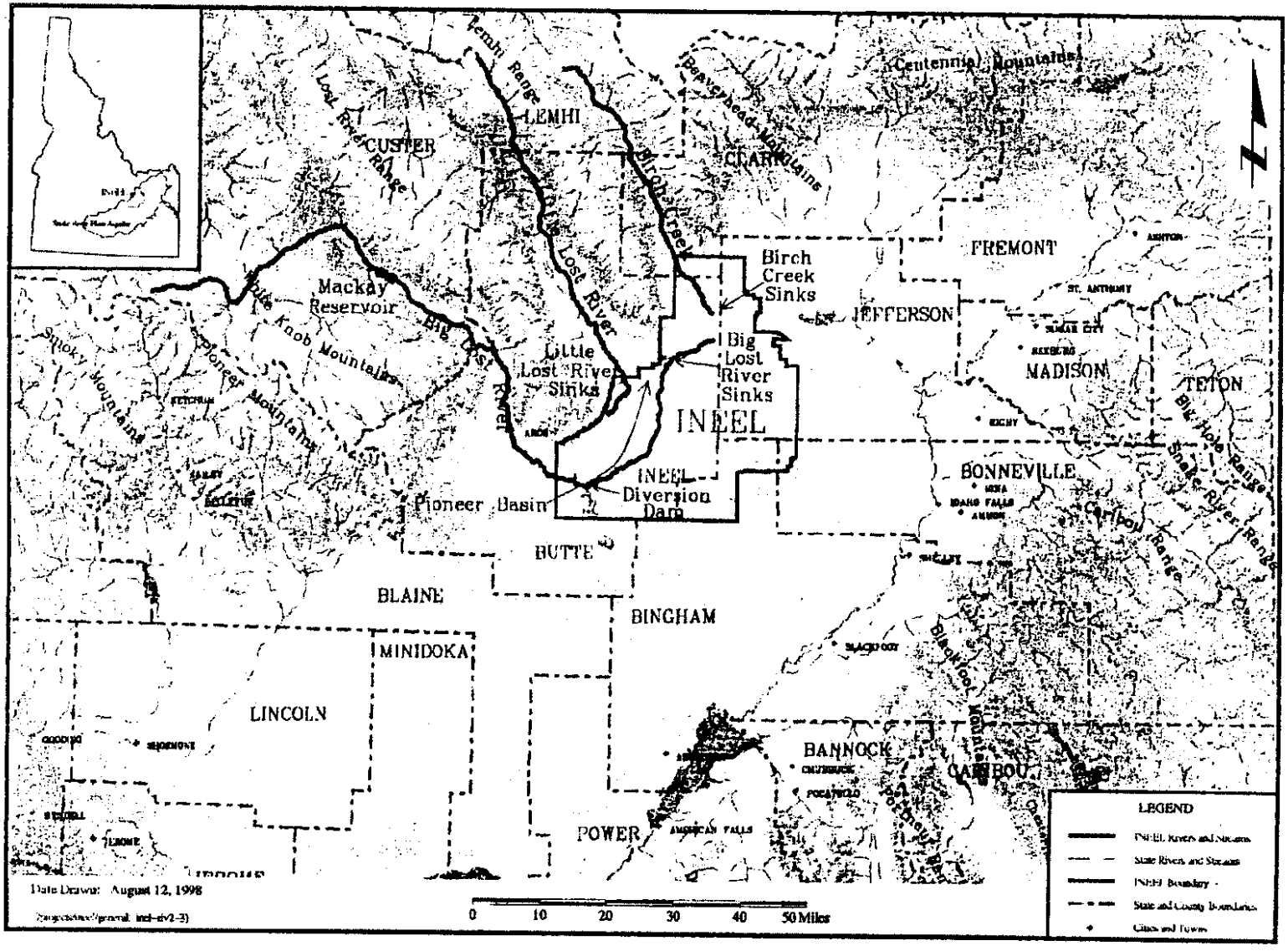

Figure 2-2. Index map of the Western Snake River Plain (modified from Hackett et al. 1982).

2.2 Meteorology

Atmospheric transport of contaminants is controlled by the following physical parameters: particle size, climate, local meteorology, local topography, large structures or buildings onsite, and contaminant source strength. This section describes the physical parameters that are necessary to evaluate environmental and human health impacts from atmospheric transportation of contaminants from CFA.

2.2.1 Climate

In 1949, the U.S. Weather Bureau, under agreement with DOE, established a complete Weather Bureau Station at the INEEL (then the NRTS). Wind direction, speed, temperature, and precipitation have been continuously recorded at CFA since approximately 1949. Most of the information presented in this section is summarized from the 2nd edition of *Climatography of the Idaho National Engineering Laboratory* (Clawson, Start, and Ricks 1989), which compiles results of weather recordings from 1949 to 1988. Further details of the INEEL's meteorology can be obtained from this reference. The longest and most complete record of meteorological observations at the INEEL is kept at the CFA station.

The climate at the INEEL is influenced by the regional topography and upper-level wind patterns over North America. The Rocky Mountains and the ESRP help to create a semi-arid climate with an average summer day-time maximum temperature of 28°C (83°F) and an average winter day time maximum temperature of -0.5°C (31°F). Infrequent cloud cover over the region allows intense solar heating of the ground surface during the day, and the low absolute humidity allows significant radiant cooling at night. These factors create large temperature fluctuations near the ground (Bowman et al. 1984). During a 22-year period of meteorological records (1954 through 1976), temperature extremes at the INEEL have varied from a low of -45°C (-49°F) in January to a high of 39°C (103°F) in July.

2.2.2 Local Meteorology

The average relative humidity at the INEEL ranges from a monthly average minimum of 15% in August to a monthly average maximum of 81% in February and December. The relative humidity is directly related to diurnal temperature fluctuations. Relative humidity reaches a maximum just before sunrise (the time of lowest temperature) and a minimum in the late afternoon (time of maximum daily temperature) (Van Deusen and Trout 1990).

Average annual precipitation at the INEEL is 21.5 cm (8.5 in.). The highest precipitation rates occur during the months of May and June and the lowest precipitation rates occur in July. Snowfall at the INEEL ranges from a low of approximately 30.5 cm (12 in.) per year to a high of approximately 127 cm (40 in.) per year, with an annual average of 66 cm (26 in.). Normal winter snowfall occurs from November through April, although occasional snowstorms occur in May, June, and October (Van Deusen and Trout 1990).

A statistical analysis of precipitation data from CFA for the period 1950 through 1990 was performed to determine estimates for the 25- and 100-year maximum 24-hour precipitation amounts and the 25- and 100-year maximum snow depths (Sagendorf 1991). Results from this study indicate 3.43 cm (1.35 in.) of precipitation for a 25-year, 24-hour storm event, and 4.1 cm (1.6 in.) of precipitation for a 100-year, 24-hour storm event. The expected 25-year maximum snow depth is 57.4 cm (22.6 in.) and the 100-year maximum snow depth is 77.8 cm (30.6 in.).

Potential annual evaporation from saturated ground surface at the INEEL is approximately 91 cm (36 in.). Eighty percent of this evaporation occurs between May and October. During the warmest month (July), the potential daily evaporation rate is approximately 0.63 cm/day (0.25 in./day). During the coldest months (December through February), evaporation is low and may be insignificant. Actual evapotranspiration by native vegetation on the INEEL parallels the total annual precipitation input.

The local meteorology is influenced by local topography, mountain ranges, and large-scale weather systems. The orientation of the bordering mountain ranges and the general orientation of the ESRP play an important role in determining the wind regime. The INEEL is in the belt of prevailing westerly winds, which are normally channeled across the ESRP. This channeling usually produces a west-southwest or southwest wind. When the prevailing westerlies at the gradient level (approximately 1,500 m [5,000 ft] above land surface) are strong, the winds channeled across the ESRP between the mountains become very strong. Some of the highest wind speeds at the INEEL have been observed under these meteorological conditions. The greatest frequency of high winds occur mainly in the spring. Average monthly wind speeds up to 6 m (20 ft) in height are highest in the month of April with speeds of 15 km/h (9 mph) at CFA. The highest wind speeds recorded at CFA and Test Area North (TAN) are 108 km/h (67 mph) and 100 km/h (62 mph), respectively.

The INEEL is subject to severe weather episodes throughout the year. Thunderstorms are observed mostly during the spring and summer. An average of two to three thunderstorms occur during June, July, and August. Thunderstorms may be accompanied by strong, gusty winds that may produce local dust storms. Precipitation from thunderstorms at the INEEL is generally light. Dust devils are also common in the region. Dust devils can entrain dust and pebbles and transport them over short distances. This usually occurs on warm sunny days with little or no wind. The dust cloud may be several hundred yards in diameter and extend several hundred feet in the air.

The vertical temperature and humidity profiles in the atmosphere determine the atmospheric stability. Stable atmospheres are characterized by low levels of turbulence and less vertical mixing. This results in higher ground level concentrations of emitted contaminants. The stability parameters at the INEEL range from extremely stable to very unstable. The stable conditions occur mostly at night during strong radiant cooling. Unstable conditions can occur during the day when there is strong solar heating of the surface layer or whenever a synoptic scale disturbance passes over the region.

2.3 Geology

The geology of the INEEL is strongly influenced by volcanic and seismic processes which have created the ESRP and the surrounding basin and range structures. The current theory of the evolution of the ESRP volcanic province is that it was formed in response to movement of the North American continent over a deep-seated plume of anomalously hot mantle rocks (hotspot) that now resides beneath Yellowstone National Park (Armstrong et al. 1975, Pierce and Morgan 1992). Movement of the continent and northeast-directed extension of the crust caused both the ESRP and the northeastern Basin-and-Range province to develop during the past 17 million years. During that time, extension of the crust has produced northwest trending normal faults and mountain ranges, while volcanic activity associated with the Yellowstone Plateau hotspot has produced a belt of calderas along the ESRP. The Yellowstone hotspot was beneath the INEEL area approximately 6.5 to 4.3 million years ago and produced the volcanic fields shown in Figure 2-3. The Pleistocene calderas of the Yellowstone Plateau formed from 2.1 to 0.6 million years ago, and strong geothermal activity continues as the hotspot still resides beneath the Yellowstone Plateau.

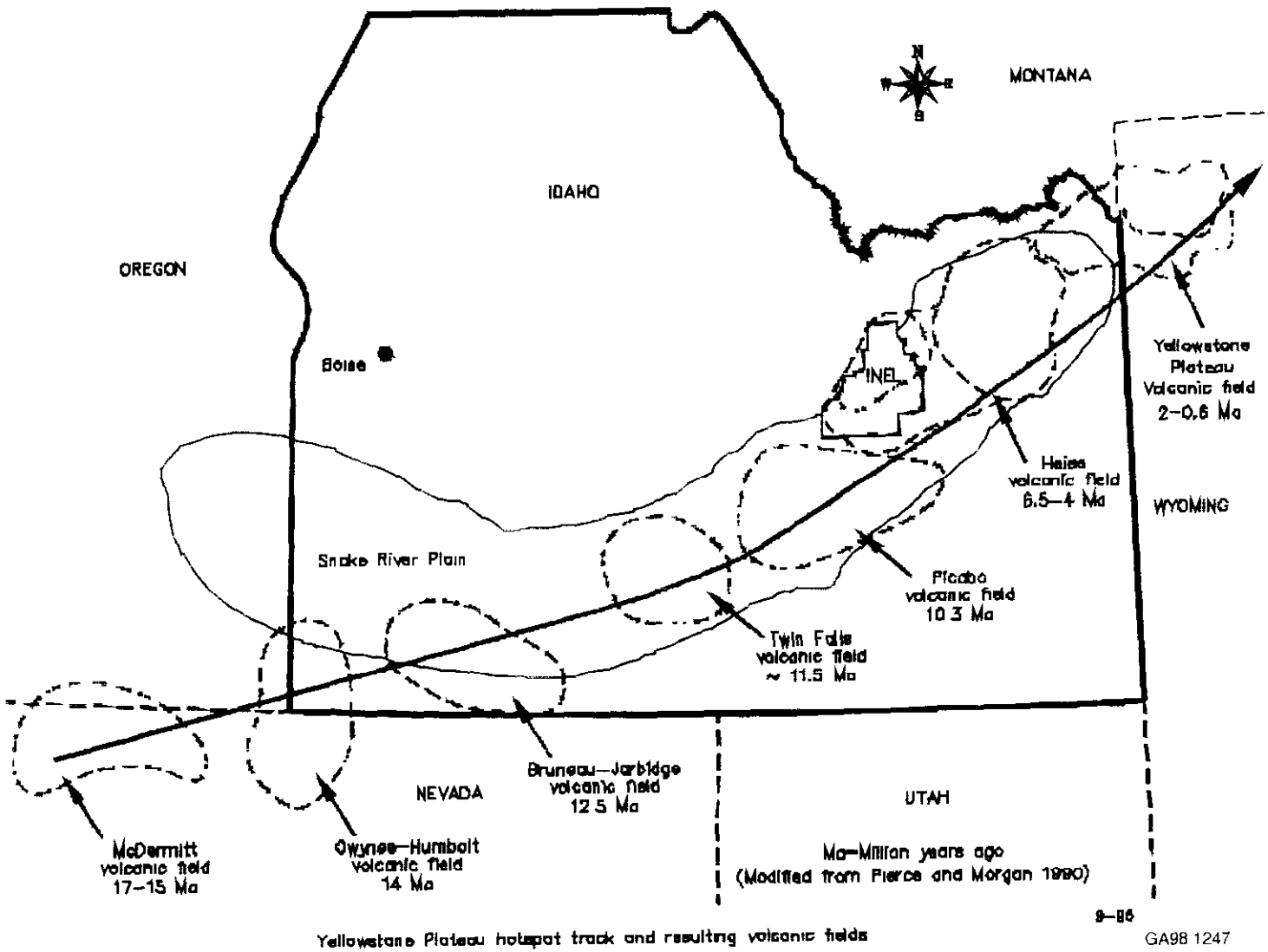

Figure 2-3. Yellowstone Plateau hotspot track and resulting volcanic fields (AC3090).

2.3.1 Regional Geology

The Lemhi, Beaverhead, and Lost River mountain ranges are located north of the ESRP (refer to Figure 2-2). These ranges are composed of Paleozoic sedimentary rocks that were folded and faulted along the northeastward-trending axis during late Cretaceous or early Tertiary Laramide Orogeny. Many of these Paleozoic rocks dip toward the axis of the ESRP (Nace et al. 1975). Within the margins of the ESRP, Miocene and younger volcanic rocks rest unconformably on deformed or tilted sedimentary and plutonic rocks ranging in age from Precambrian to Mesozoic and on faulted remnants of middle to late Eocene "calcalkalic" volcanic rocks (Leeman 1982).

Much of the INEEL is covered by unconsolidated surficial deposits of various ages and origins. A wide band of Quaternary alluvium extends along the course of the Big Lost River from the southwestern corner of INEEL to the Lost River Sinks in the north-central portion of the INEEL. Lacustrine (lake) deposits of clays, silts, and sands deposited in Pleistocene Lake Terreton occur in the northern part of INEEL. Wind deposited silts or loess with thicknesses of up to approximately 6 m (20 ft) cover much of the basalt bedrock at the INEEL. Beach sands deposited at the high stand of Lake Terreton were reworked by winds in the late Pleistocene and Holocene time and form large dune fields (eolian deposits) in the northeastern portion of the INEEL (Scott 1982). Large alluvial fans occur in limited areas along the northwest and west boundaries of the INEEL at the base of the Arco hills and the Lemhi Range.

Because of their mechanism of eruption, flow from the source vents, and cooling after emplacement the basalt lava flows possess predictable vertical and horizontal facies distributions (Figure 2-4). From bottom to top, basalt lava flows are typically composed of a basal rubble zone, a lower vesicular zone, a massive columnar jointed zone, an upper vesicular and fissured zone, and a cap of platy jointed crust. From source to distal end, the flows grade from thin, cavernous, platy flows (shelly pahoehoe) with interlayered pyroclastic material, to thick units with the vertical zoning described above. In the medial and distal areas, deflation depressions or pits are common and fissures in the broken crust are numerous. Many of the lava flows (especially the larger ones) on the ESRP are fed by lava tubes that commonly drain in the late stages of eruption, leaving long openings in the flows. In the lava flow sequence beneath the ESRP and the INEEL, the basal rubble zones, cooling fractures, fissures, lava tubes, vesicles, cavernous shelly pahoehoe, and pyroclastic zones furnish the porosity and permeability for the storage and transport of water in the aquifer. All of these features are primary (i.e., they were formed during emplacement of the rocks) except the polygonal cooling fractures.

Because of the concentration of volcanic activity along the Axial Volcanic Zone (Figure 2-5) and along volcanic rift zones, these areas tend to be constructional highlands that receive less sediment than other areas. Thus, the total thickness of sediments in the basalt and sediment sequence tends to be greater near the plain margins (Whitehead 1986) and between volcanic rift zones. In fact, many of the drill holes along the Axial Volcanic Zone show that no interbeds occur in that area. The combination of sparse interbeds, and abundance of shelly pahoehoe and pyroclastic material along the Axial Volcanic Zone suggest a thicker and more actively moving aquifer there than elsewhere on the ESRP.

In conclusion, Bartholomay (1990) found that the mineralogy of sedimentary interbeds in the Radioactive Waste Management Complex (RWMC), Test Reactor Area (TRA), and Idaho Nuclear Technology and Engineering Center (INTEC, formerly the Idaho Chemical Processing Plant [ICPP]) areas correlate with sediments of the Big Lost River drainage, and the mineralogy of sedimentary interbeds at TAN correlates with surficial deposits of the Birch Creek drainage. These correlations suggest that the sedimentary interbeds probably were deposited in a depositional environment similar to present-day conditions.

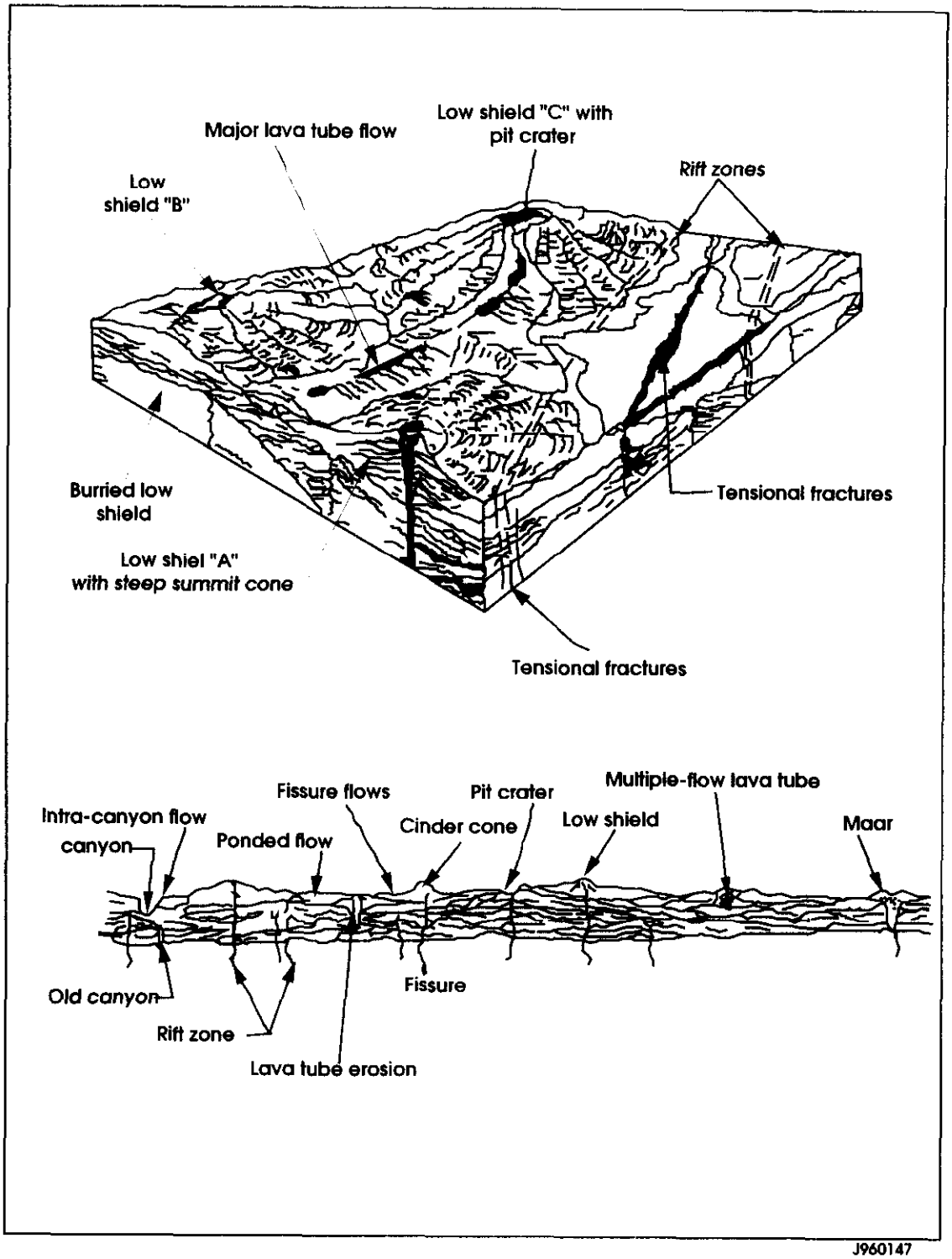

Figure 2-4. Block diagram showing the relationship of low shields, major lava tube flows and fissure flows (J960147).

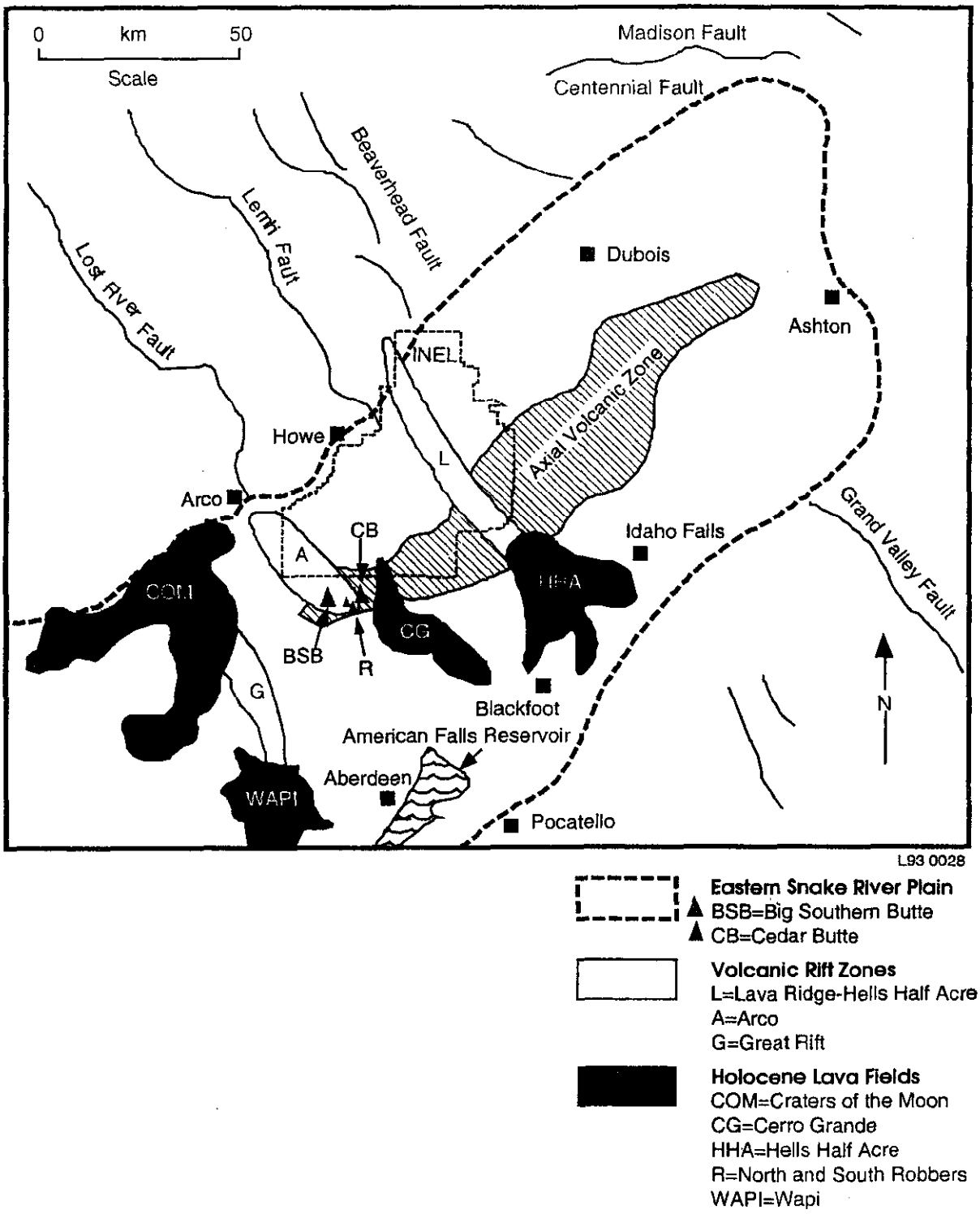

Figure 2-5. Illustration of the axial volcanic zone (L93 0028).

2.3.2 Geology of WAG 4

WAG 4 sits on Big Lost River alluvial deposits (Figure 2-6). The alluvial deposits are underlain by thick sequences of interfingering basalt lava flows and thin sedimentary interbeds, as shown in the geologic cross sections taken from well log data (Figure 2-7). The sequence of basalt flows and interbedded sediments extends well below the water table to a depth of several thousand feet. Basalt lava-flow groups, separated by sedimentary interbeds, are composed of numerous basalt lava flows that erupted from one or more vents. From bottom to top, each lava flow is typically composed of a basal zone of highly permeable rubble; a lower vesicular zone; a dense, massive, and jointed central zone; an upper vesicular zone; and a cap of slabby lava crust. Considerable variation occurs in the characteristics of the basalts. The basalts may be fine or coarse-grained, vesicular or nonvesicular, fractured or jointed. Some fractures and vesicles may be filled with sedimentary material or secondary calcite.

Interbedded sediments consist predominantly of fine-grained silts of eolian origin and clays, silts, sands, and relatively uncommon gravels deposited by streams such as the Big Lost River. Subsurface sedimentary interbeds are lithologically similar to surficial sediments, and past depositional processes and systems are therefore inferred to have been similar to those of recent times. Physical and properties of a shallow sedimentary interbed beneath the CFA Landfills II and III are shown in Table 2-1 (Stephens and Associates 1993). The samples from the interbed tend to be coarse-textured with correspondingly low cation exchange capacity (CEC) and carbon contents. However, physical property variability is evident even in samples collected near each other (e.g., silt and clay contents of samples from wells LF2-12 and LF2-12A). Such variability is also evident over wider distance scales at the INEEL. Grain-size distributions and CECs of sedimentary material from interbeds and basalt fracture fill have been determined at the RWMC a little over 11 km (7 mi) from CFA (Barraclough et al. 1976; Rightmire 1984). Interbed sediments are generally about 60% silt and clay, 35% sand, and 5% gravel. The 34-m (110-ft) interbed at the RWMC is somewhat coarser (10% gravel, 45% sand, 45% silt and clay) than the 73-m (240-ft) interbed (2% gravel, 28% sand, 70% silt and clay). Fracture-fill material in the basalts averaged 22% gravel, 25% sand, and 53% silt and clay.

CEC of the 9-, 34-, and 73-m (30-, 110-, and 240-ft) interbeds at the RWMC averaged 9.0, 7.6, and 15.4 meq/100 g, respectively. The CEC of the fracture-fill sediments was 13.6 and 16.1 meq/100 g for material collected from depths less than 34 m (110 ft) and from the depth interval 34 to 73 m (110 to 240 ft), respectively. Additional variations also occur among the sedimentary interbeds. Some interbeds are continuous beneath the area of the landfills, while others are thin and discontinuous. Some interbeds may also be compacted due to original deposition and subsequent overburden pressures.

Interbeds with relatively high clay content may provide some measure of defense against the possible migration of contaminant leachate from WAG 4 release sites. Such interbeds will impede the downward migration of water and contaminants to the water table by virtue of their very low permeability and high adsorptive capacity. However, many of the interbeds shown in Figure 2-7 and observed in wells at the landfills are thin and discontinuous, confounding subsurface correlations between drill holes. Table 2-2 indicates the depths of interbed clay as observed in the field during drilling of monitoring wells around Landfills II and III. Additionally, there are local pockets or lenses of sand, silt, and clay within the lava flows that were deposited in topographic lows during periods of minimal volcanic activity.

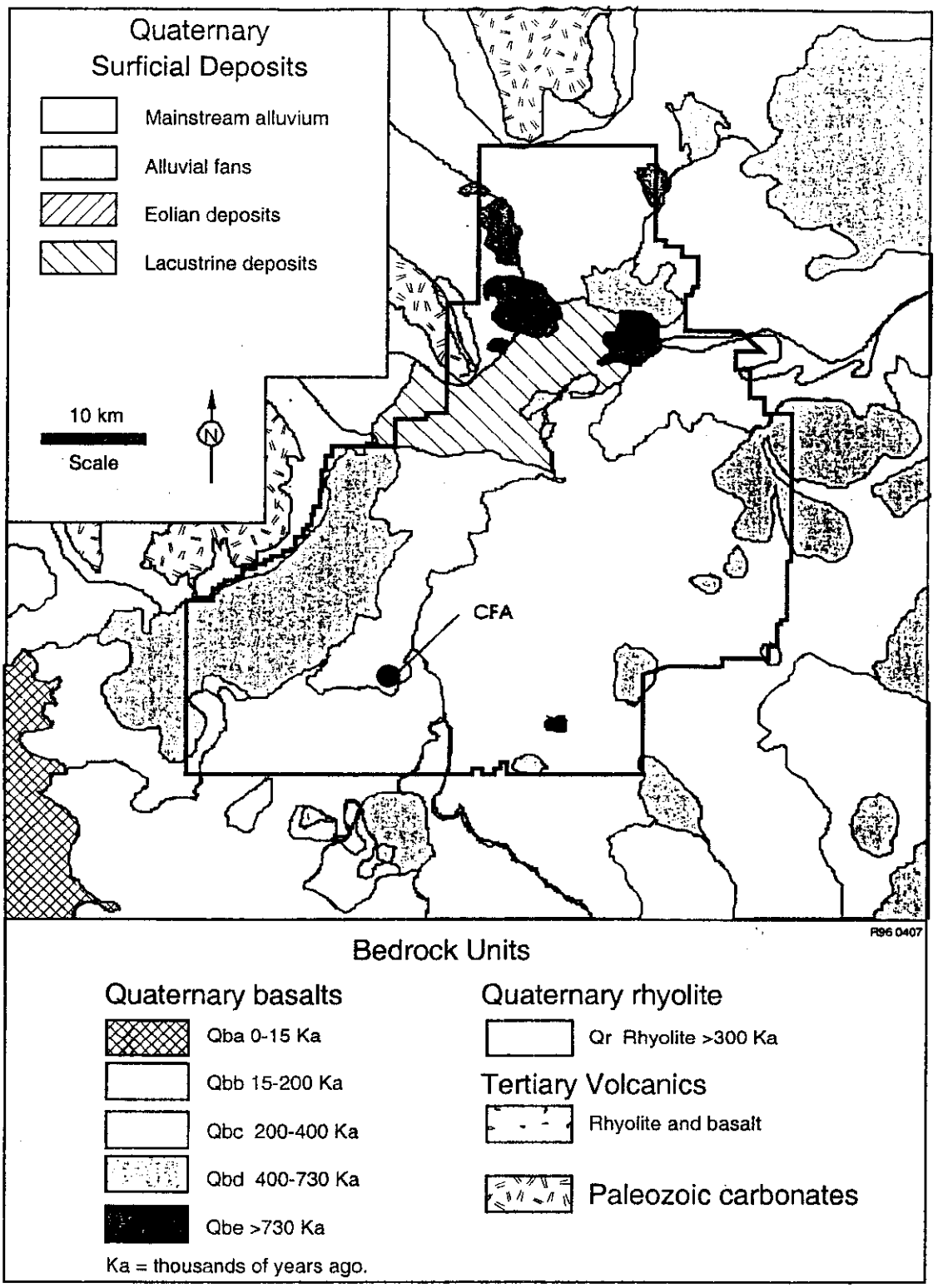

Figure 2-6. Generalized geologic map of the INEEL area, showing CFA in relation to the surficial distribution of major basalt-lava-flow groups and sedimentary deposits (Kuntz et al. 1990, Scott 1982) (R960407).

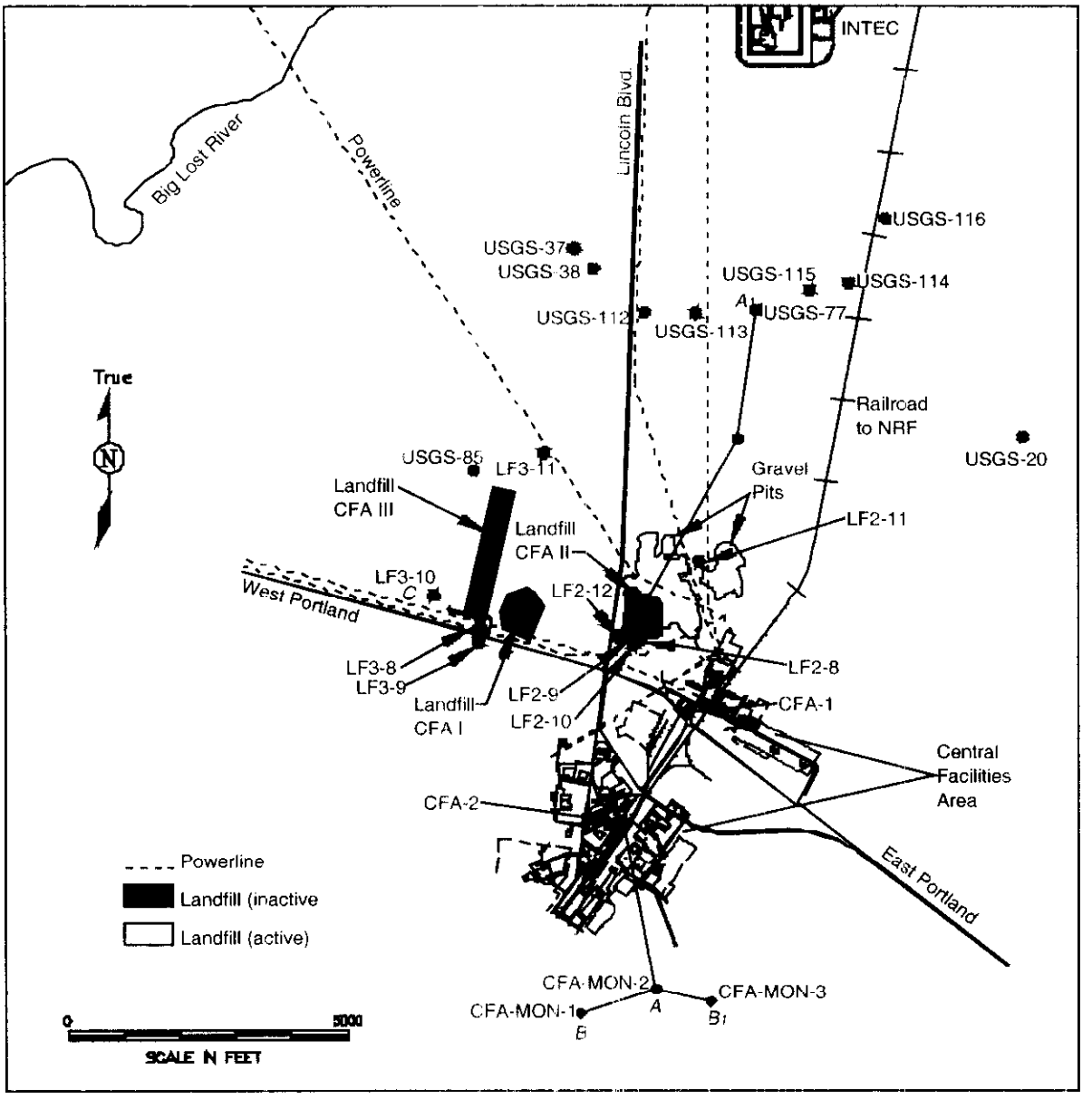

Figure 2-7. Stratigraphic cross sections in the vicinity of the CFA landfills.

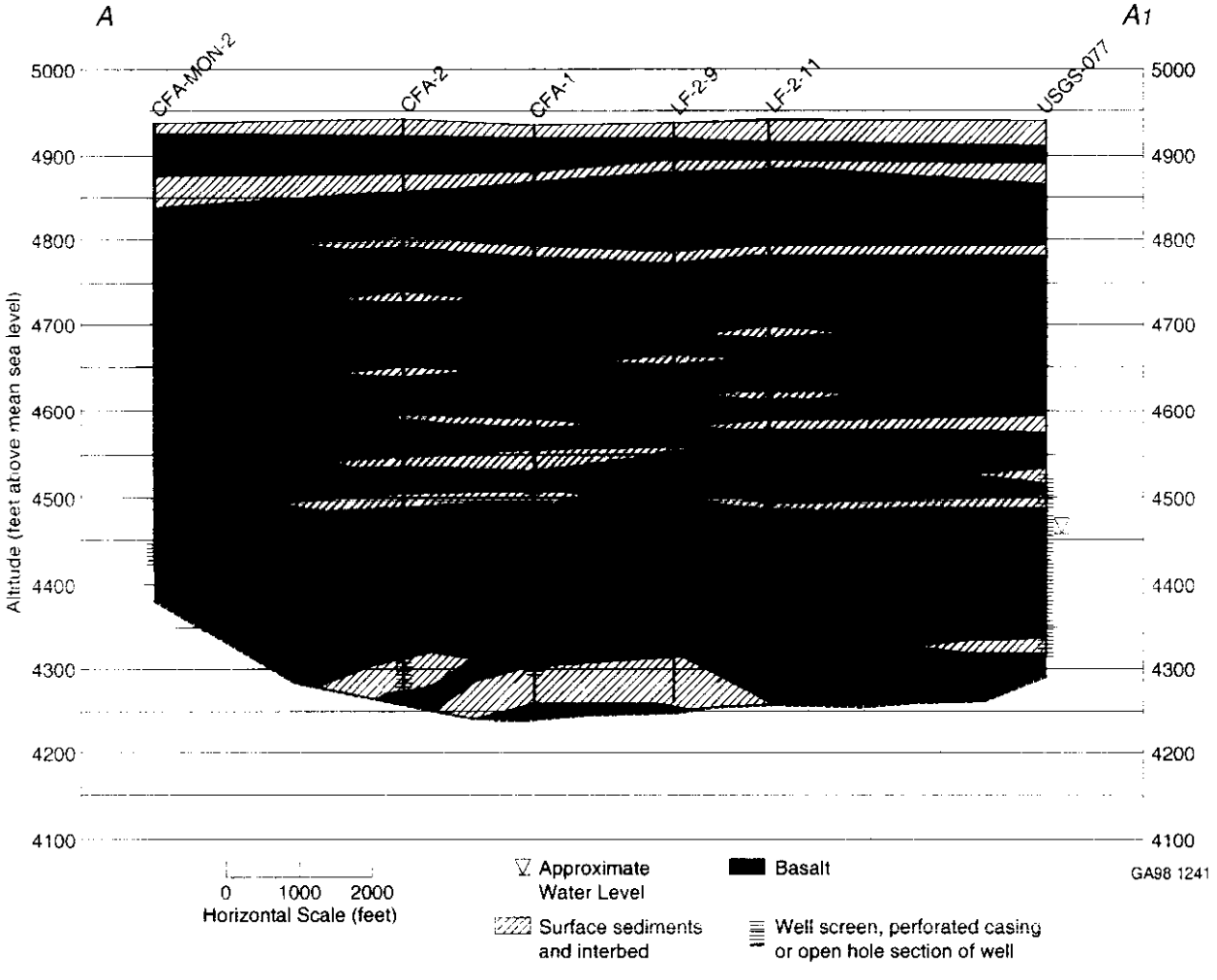

Figure 2-7. (continued).

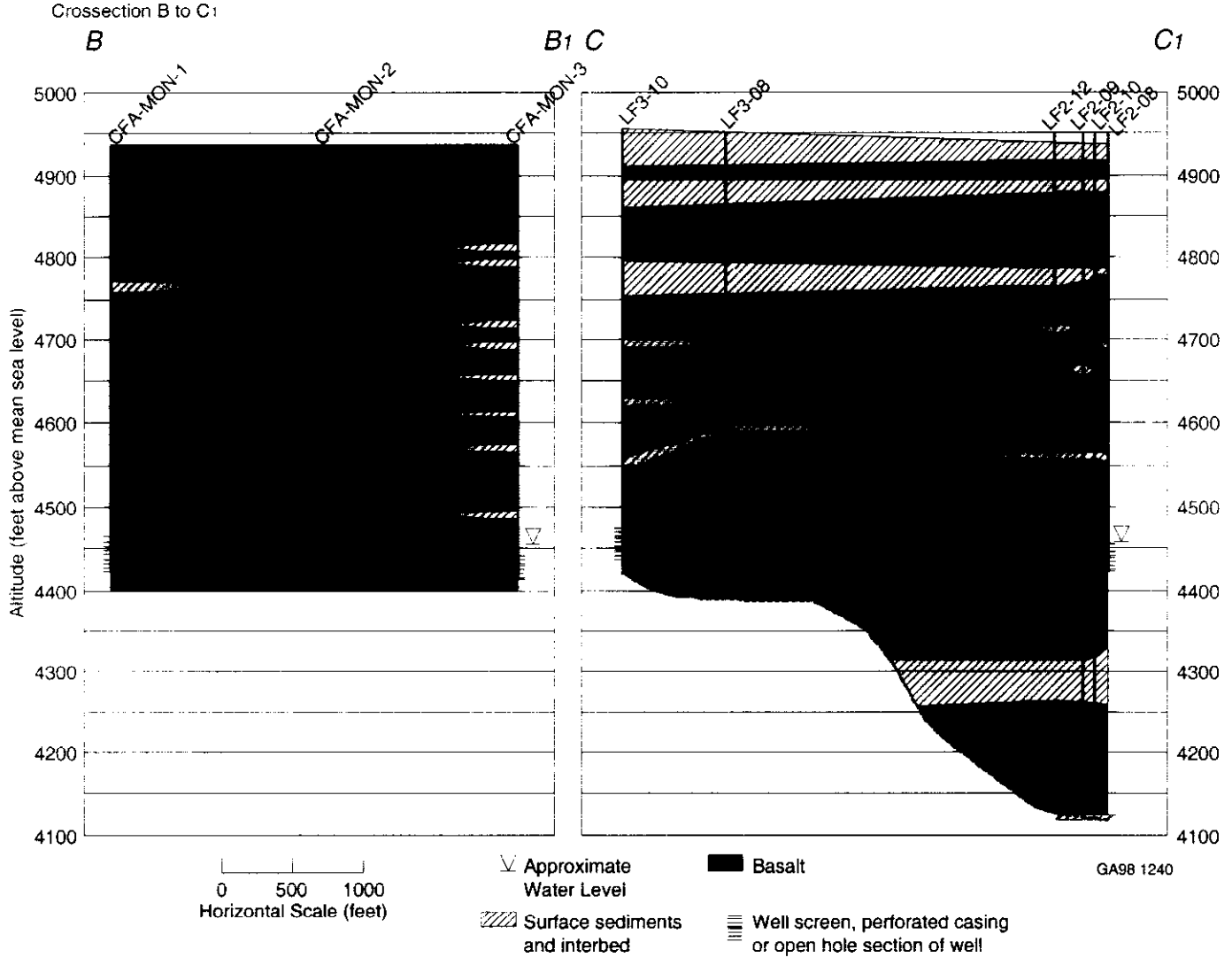

Figure 2-7. (continued).